



Article

# Differential Effects of the Betablockers Carvedilol, Metoprolol and Bisoprolol on Cardiac $K_v4.3$ ( $I_{to}$ ) Channel Isoforms

Ann-Kathrin Rahm <sup>1,2,3,\*</sup>, Juline Hackbarth <sup>1,2,†</sup>, Mara E. Müller <sup>1,2,3</sup>, Julia Pfeiffer <sup>1,2</sup>, Heike Gampp <sup>1,2</sup>, Finn Petersenn <sup>1,2</sup>, Rasmus Rivinius <sup>1,2</sup>, Norbert Frey <sup>1,2,3</sup>, Patrick Lugenbiel <sup>1,2,3</sup> and Dierk Thomas <sup>1,2,3</sup>

<sup>1</sup> Heidelberg Center for Heart Rhythm Disorders, Heidelberg University Hospital, 69120 Heidelberg, Germany; mara.mueller@med.uni-heidelberg.de (M.E.M.); rasmus.rivinius@med.uni-heidelberg.de (R.R.); patrick.lugenbiel@med.uni-heidelberg.de (P.L.)

<sup>2</sup> Department of Cardiology, Heidelberg University Hospital, 69120 Heidelberg, Germany

<sup>3</sup> DZHK (German Center for Cardiovascular Research), Partner Site Heidelberg/Mannheim, 69120 Heidelberg, Germany

\* Correspondence: ann-kathrin.rahm@med.uni-heidelberg.de

† These authors contributed equally to this work.

**Abstract:** Cardiac  $K_v4.3$  channels contribute to the transient outward  $K^+$  current,  $I_{to}$ , during early repolarization of the cardiac action potential. Two different isoforms of  $K_v4.3$  are present in the human ventricle and exhibit differential remodeling in heart failure (HF). Cardioselective betablockers are a cornerstone of HF with reduced ejection fraction therapy as well as ventricular arrhythmia treatment. In this study we examined pharmacological effects of betablockers on both  $K_v4.3$  isoforms to explore their potential for isoform-specific therapy.  $K_v4.3$  isoforms were expressed in *Xenopus laevis* oocytes and incubated with the respective betablockers. Dose-dependency and biophysical characteristics were examined. HEK 293T-cells were transfected with the two  $K_v4.3$  isoforms and analyzed with Western blots. Carvedilol (100  $\mu$ M) blocked  $K_v4.3$  L by  $77 \pm 2\%$  and  $K_v4.3$  S by  $67 \pm 6\%$ , respectively. Metoprolol (100  $\mu$ M) was less effective with inhibition of  $37 \pm 3\%$  ( $K_v4.3$  L) and  $35 \pm 4\%$  ( $K_v4.3$  S). Bisoprolol showed no inhibitory effect. Current reduction was not caused by changes in  $K_v4.3$  protein expression. Carvedilol inhibited  $K_v4.3$  channels at physiologically relevant concentrations, affecting both isoforms. Metoprolol showed a weaker blocking effect and bisoprolol did not exert an effect on  $K_v4.3$ . Blockade of repolarizing  $K_v4.3$  channels by carvedilol and metoprolol extend their pharmacological mechanism of action, potentially contributing beneficial antiarrhythmic effects in normal and failing hearts.

**Keywords:**  $K_v4.3$ ;  $I_{to}$ ; betablocker; antiarrhythmic effects; heart failure



**Citation:** Rahm, A.-K.; Hackbarth, J.; Müller, M.E.; Pfeiffer, J.; Gampp, H.; Petersenn, F.; Rivinius, R.; Frey, N.; Lugenbiel, P.; Thomas, D. Differential Effects of the Betablockers Carvedilol, Metoprolol and Bisoprolol on Cardiac  $K_v4.3$  ( $I_{to}$ ) Channel Isoforms. *Int. J. Mol. Sci.* **2023**, *24*, 13842. <https://doi.org/10.3390/ijms241813842>

Academic Editor: Anindita Das

Received: 30 July 2023

Revised: 3 September 2023

Accepted: 5 September 2023

Published: 8 September 2023



**Copyright:** © 2023 by the authors. Licensee MDPI, Basel, Switzerland. This article is an open access article distributed under the terms and conditions of the Creative Commons Attribution (CC BY) license (<https://creativecommons.org/licenses/by/4.0/>).

## 1. Introduction

The cardiac  $K_v4.3$  channel is the main carrier of the transient outward potassium current ( $I_{to}$ ) during the early repolarization phase of the cardiac action potential [1]. Changes in expression and function of this channel are associated with cardiac conditions such as Brugada syndrome, atrial fibrillation, and early repolarization syndrome. Moreover,  $K_v4.3$  expression changes have been reported after myocardial infarction and heart failure (HF) [2–4]. A consistent electrophysiological feature in HF is a prolongation of the ventricular action potential [5,6]. In animal HF models, as well as in human cardiac myocytes, a reduction of the transient outward potassium current in the early repolarization phase mediated by  $K_v4.3$  was observed [7–11]. The cardiac  $K_v4.3$  channel, which is encoded by the *KCND3* gene, is activated voltage dependently. There are two different isoforms that result from the alternative splicing of exon 6. The longer  $K_v4.3$  L variant and the shorter isoform  $K_v4.3$  S differ in a 19 amino acid long sequence at the intracellular C-terminus [12,13]. In patients with dilated cardiomyopathy expression levels of  $K_v4.3$ , isoforms are differentially

expressed:  $K_v4.3$  L is upregulated, whereas  $K_v4.3$  S is downregulated. As a result, the long isoform is predominantly expressed in the insufficient heart [4].

Betablockers constitute a cornerstone of pharmacological HF therapy [14]. Metoprolol, bisoprolol and carvedilol reduced mortality in HF patients [15–17]. Betablockers attenuate the proarrhythmic effect of catecholamines, which are pathologically elevated in HF. They exert negative ino-, chrono-, dromo-, and bathmotropic effects and directly affect ventricular remodeling through alterations in expression and function of ion channels. In particular, carvedilol interacts with cardiac ion channels, including human ether-a-go-go-related gene (hERG)  $K^+$  channels and two-pore-domain potassium channels ( $K_{2P}$ ) [18–22].

The aim of this study was to examine differential effects of carvedilol, bisoprolol, and metoprolol on  $K_v4.3$  isoforms to provide the basis for isoform-specific HF drug therapy.

## 2. Results

### 2.1. Effects of Carvedilol on the Function of $K_v4.3$ Channel Isoforms

Carvedilol caused time-dependent inhibition of the  $K_v4.3$  peak current. Both isoforms were similarly affected. Maximum inhibitory effects observed after 50 min yielded a current block of  $76.6 \pm 2.0\%$  ( $K_v4.3$  L,  $n = 8$ ,  $p < 0.001$ ) and  $67.1 \pm 5.7\%$  ( $K_v4.3$  S,  $n = 8$ ,  $p < 0.001$ ).  $K_v4.3$  currents before and after application of carvedilol, as well as the development of the block, are shown in Figure 1A–D.

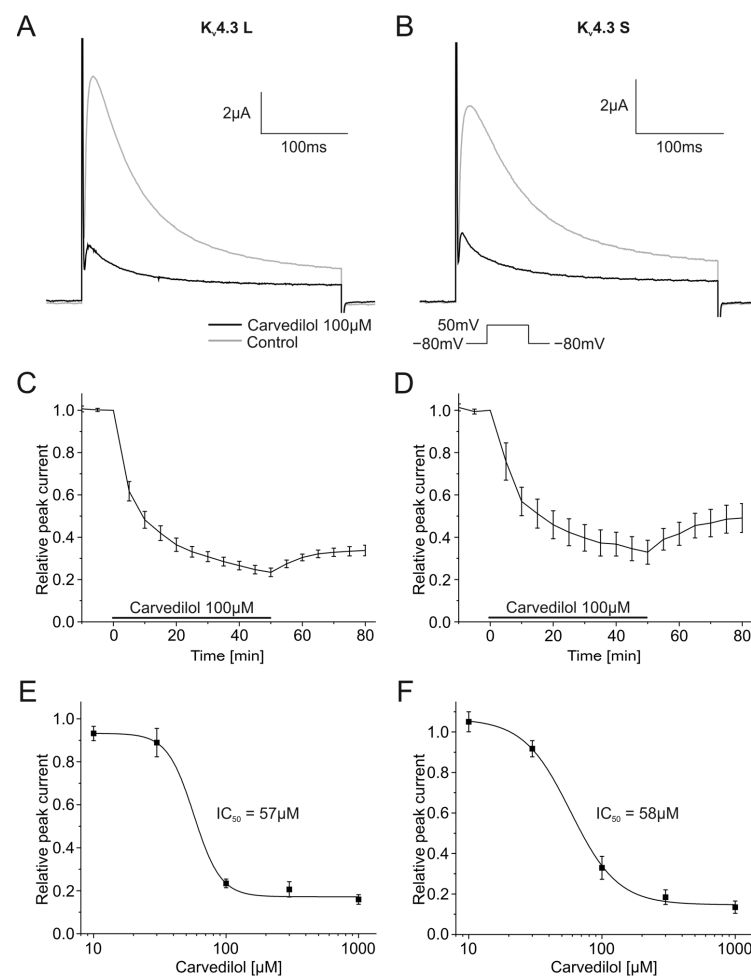


**Figure 1.** Effects of carvedilol (100  $\mu$ M) on currents produced by the  $K_v4.3$  isoform. (A,B) Representative current traces of  $K_v4.3$  L (A) and  $K_v4.3$  S (B) prior to (gray) and after (black) carvedilol application (50 min). (C,D) Relative peak current of  $K_v4.3$  L ( $n = 8$ ) (C) and  $K_v4.3$  S ( $n = 8$ ) (D) before, during and after the application 100  $\mu$ M carvedilol. (E,F) Concentration-response curves for  $K_v4.3$  L ( $n = 8$ –12) ( $IC_{50} = 57.1 \pm 12.6$   $\mu$ M) (E) and  $K_v4.3$  S ( $n = 8$ –13) ( $IC_{50} = 58.2 \pm 6.2$   $\mu$ M) (F).

The inhibition of  $K_v4.3$  L and  $K_v4.3$  S currents was partially reversible. The peak current returned to  $33.8 \pm 2.6\%$  for the L isoform, and  $49.1 \pm 6.8\%$  for the S isoform after 30 min wash out. Blockade was concentration dependent with  $IC_{50}$  values of  $57.1 \pm 12.6 \mu\text{M}$  ( $K_v4.3$  L,  $n = 8-12$ ) and  $58.2 \pm 6.2 \mu\text{M}$  ( $K_v4.3$  S,  $n = 8-13$ ) (Figure 1E,F).

## 2.2. Biophysical Characteristics of $K_v4.3$ Inhibition by Carvedilol

Activation and inactivation kinetics were assessed by applying depolarizing steps from  $-100$  mV to  $+50$  mV (2000 ms, 10 mV increments) from a holding potential of  $-80$  mV. There was a return pulse to  $+50$  mV after the first voltage step. The double-step voltage protocol as well as typical current traces in the absence and the presence of  $100 \mu\text{M}$  carvedilol are depicted in Figure 2A,B.

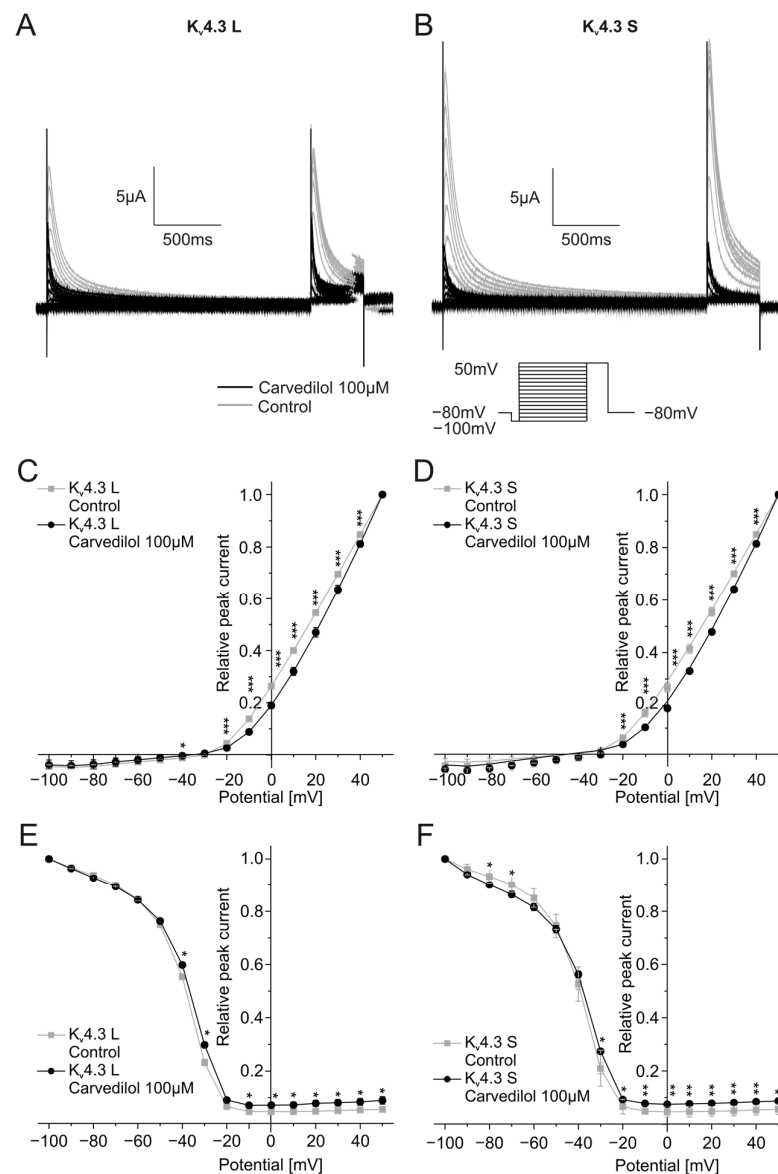


**Figure 2.** Effects of carvedilol ( $100 \mu\text{M}$ ) on activation and inactivation of the  $K_v4.3$  isoforms. (A,B) Representative current traces of  $K_v4.3$  L (A) and S (B) evoked by the indicated voltage protocol prior to (gray) and after (black) carvedilol application (50 min). (C,D) I-V-plots for activation of  $K_v4.3$  L (C) and  $K_v4.3$  S (D) ( $n = 11$ ). (E,F) I-V-plots for inactivation of  $K_v4.3$  L (E) and  $K_v4.3$  S (F) ( $n = 11$ ). \*  $p < 0.05$ , \*\*  $p < 0.01$ , \*\*\*  $p < 0.001$ .

To examine the effects of carvedilol on  $K_v4.3$  channel activation, peak currents measured during the first part of the voltage protocol were normalized to the peak current of the last trace and then plotted against the test pulse voltage. Application of carvedilol led to a shift of the half-maximal activation voltages of both  $K_v4.3$  isoforms towards more positive voltages. The half-maximal activation voltage in the presence of carvedilol ( $K_v4.3$  L:  $V_{1/2} = 31.3 \pm 4.0$  mV,  $n = 11$ ,  $p < 0.0001$ ,  $K_v4.3$  S:  $V_{1/2} = 32.0 \pm 3.1$  mV,  $n = 11$ ,  $p < 0.0001$ ) differed significantly from the measurements under control conditions ( $K_v4.3$  L:  $V_{1/2} = 22.6 \pm 2.3$  mV,  $n = 11$ ,  $K_v4.3$  S:  $V_{1/2} = 22.4 \pm 1.6$  mV,  $n = 11$ ) (Figure 2C,D).

The current peak evoked by the second voltage step reflects channel inactivation. Inactivation of the two  $K_v4.3$  isoforms was analyzed by plotting the peak current during the second step of the voltage protocol against the respective test pulse potential. Half-maximal inactivation voltages after application of 100  $\mu$ M carvedilol were numerically more positive compared to control conditions without reaching statistical significance.  $K_v4.3$  L half-maximal inactivation voltage was  $-39.5 \pm 1.3$  mV under control conditions and  $-38.3 \pm 1.3$  mV after incubation with carvedilol ( $n = 11$ ,  $p = 0.016$ ), whereas values obtained with  $K_v4.3$  S yielded  $-40.2 \pm 2.1$  mV under control conditions and  $-39.5 \pm 1.6$  mV after carvedilol administration ( $n = 11$ ,  $p = 0.398$ ) (Figure 2E,F).

To reflect ventricular tachyarrhythmias more closely with shorter cycle lengths, activation and inactivation kinetics were additionally analyzed by applying shorter depolarizing steps of 200 ms (Figure 3). Similar to the protocol described above, steps ranging from  $-100$  mV to  $+50$  mV were used from a holding potential of  $-80$  mV with increments of 10 mV. Typical current traces are depicted in Figure 3A,B. Activation and inactivation voltages were analyzed as described before. Half-maximal activation voltages were again significantly different between control conditions ( $K_v4.3$  L:  $V_{1/2} = 25.1 \pm 2.1$  mV,  $K_v4.3$  S:  $V_{1/2} = 24.6 \pm 2.8$  mV) and after 50 min incubation with 100  $\mu$ M carvedilol ( $K_v4.3$  L:  $V_{1/2} = 34.8 \pm 4.8$  mV,  $n = 11$ ,  $p < 0.0001$ ,  $K_v4.3$  S:  $V_{1/2} = 39.9 \pm 15.2$  mV,  $n = 11$ ,  $p = 0.010$ ) (Figure 3C,D). Furthermore, half-maximal inactivation voltages were slightly more positive after carvedilol administration compared to drug-free conditions, resembling findings obtained with longer voltage pulses. The difference was not significant for both isoforms: The half-maximal inactivation voltage of  $K_v4.3$  was  $-22.5 \pm 1.6$  mV (control) and  $-21.7 \pm 1.2$  mV after incubation with carvedilol ( $n = 11$ ,  $p = 0.123$ ). For  $K_v4.3$  S, values of  $-23.6 \pm 3.1$  mV under control conditions and  $-22.7 \pm 1.7$  mV after treatment with carvedilol ( $n = 11$ ,  $p = 0.464$ ) were calculated (Figure 3E,F).

Next, the recovery from  $K_v4.3$  inactivation was assessed using a multistep protocol. After a depolarization step from a holding potential of  $-80$  mV to  $+50$  mV for 500 ms, a return pulse to the  $-80$  mV holding potential was applied with durations ranging from 10 to 200 ms in 10 ms increments. The variable duration allowed the channel to recover from inactivation and was then followed by a 250 ms long depolarizing step from  $-80$  mV to  $+50$  mV. The peak currents recorded during the final variable voltage step were normalized to the highest peak current and then plotted against the respective duration of the preceding step. Representative traces are depicted in Figure 4A,B. Relative peak currents normalized to the highest peak current after the longest duration of the  $-80$  mV holding potentials (200 ms) did not differ between control measurements and recordings after 100  $\mu$ M carvedilol activation for 50 min. Time constants of recovery from inactivation were calculated after applying a single exponential fit (Figure 4C,D). Significant differences between time constants under control conditions ( $\tau = 267.0 \pm 25.8$  ms) and after 50 min incubation with carvedilol ( $\tau = 505.2 \pm 57.4$  ms,  $n = 10$ ,  $p = 0.002$ ) were observed with  $K_v4.3$  L. For  $K_v4.3$  S, the increase of the time constant was not significant. Time constants of  $229.1 \pm 45.3$  ms under control conditions and  $295.9 \pm 20.2$  ms in the presence of carvedilol were obtained ( $n = 10$ ,  $p = 0.094$ ).

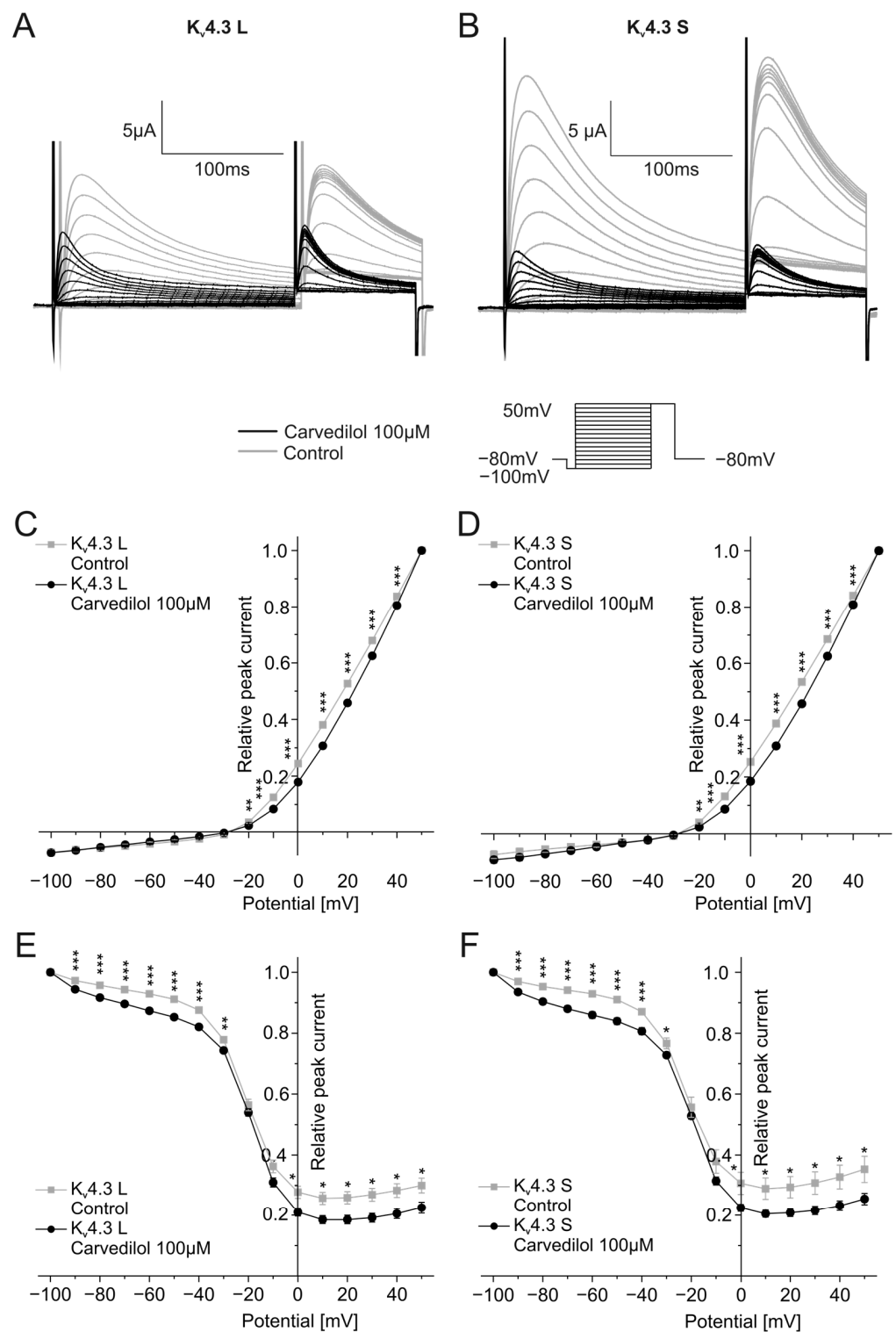


**Figure 3.** Effects of carvedilol (100  $\mu M$ ) on the activation and inactivation of the two  $K_v4.3$  isoforms with short depolarizing steps. (A,B) Representative current traces of  $K_v4.3 L$  (A) and S (B) induced by the indicated voltage protocol prior to (gray) and after (black) carvedilol application (50 min). (C,D) I-V plots for activation of  $K_v4.3 L$  (C) and  $K_v4.3 S$  (D) ( $n = 11$ ). (E,F) I-V-plots for inactivation of  $K_v4.3 L$  (E) and  $K_v4.3 S$  (F) ( $n = 11$ ). \*  $p < 0.05$ , \*\*  $p < 0.01$ , \*\*\*  $p < 0.001$ .

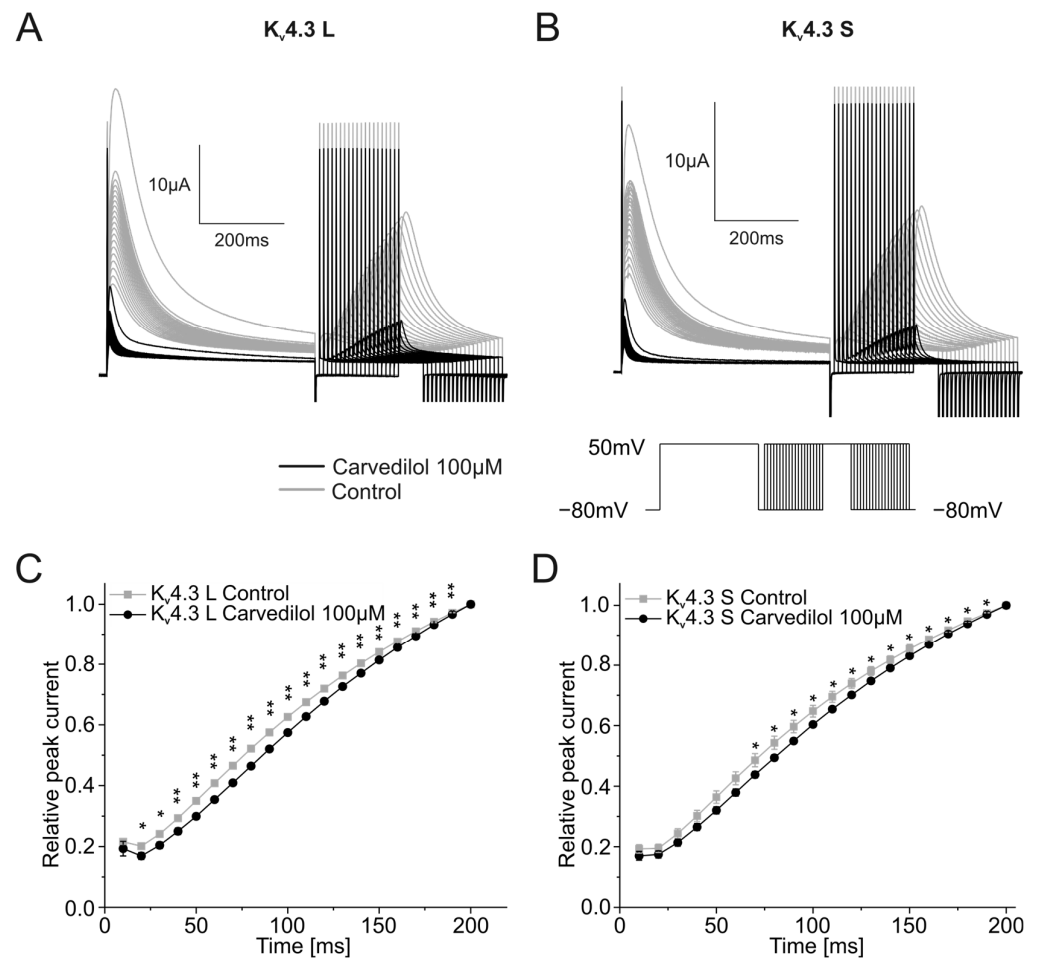


**Figure 4.** Effects of carvedilol (100  $\mu\text{M}$ ) on the recovery from inactivation of the two  $\text{K}_v4.3$  isoforms. (A,B) Representative  $\text{K}_v4.3$  L (A) and  $\text{K}_v4.3$  S (B) current traces of induced by the indicated voltage protocol prior to (gray) and after (black) carvedilol application (50 min). (C,D) Recovery from inactivation curves were calculated by plotting peak current amplitudes against the duration of the preceding repolarizing step for  $\text{K}_v4.3$  L (C) and  $\text{K}_v4.3$  S (D) ( $n = 10$ ). \*  $p < 0.05$ , \*\*  $p < 0.01$ .

Finally, channel deactivation was analyzed by briefly depolarizing the oocyte from  $-80$  mV to  $+50$  mV for 7.5 ms, followed by second 250 ms-long voltage steps ranging from  $-60$  mV to  $-30$  mV in 10 mV increments. Representative traces are shown in Figure 5A,B. Time constants of deactivation were calculated by applying single exponential fits to deactivating currents of the second part of the protocol and were then plotted against the voltage of the second pulse of the voltage protocol. Time constants showed a linear behavior. For control conditions, as well as for the measurement after incubation with 100  $\mu\text{M}$  carvedilol, channel deactivation accelerated with more negative membrane potentials (Figure 5C,D). Carvedilol caused further acceleration of channel deactivation compared to control conditions. Time constants differed significantly between the control measurements and after betablocker incubation for both channel isoforms ( $n = 11$ ,  $p < 0.001$ ) (Figure 5C,D).

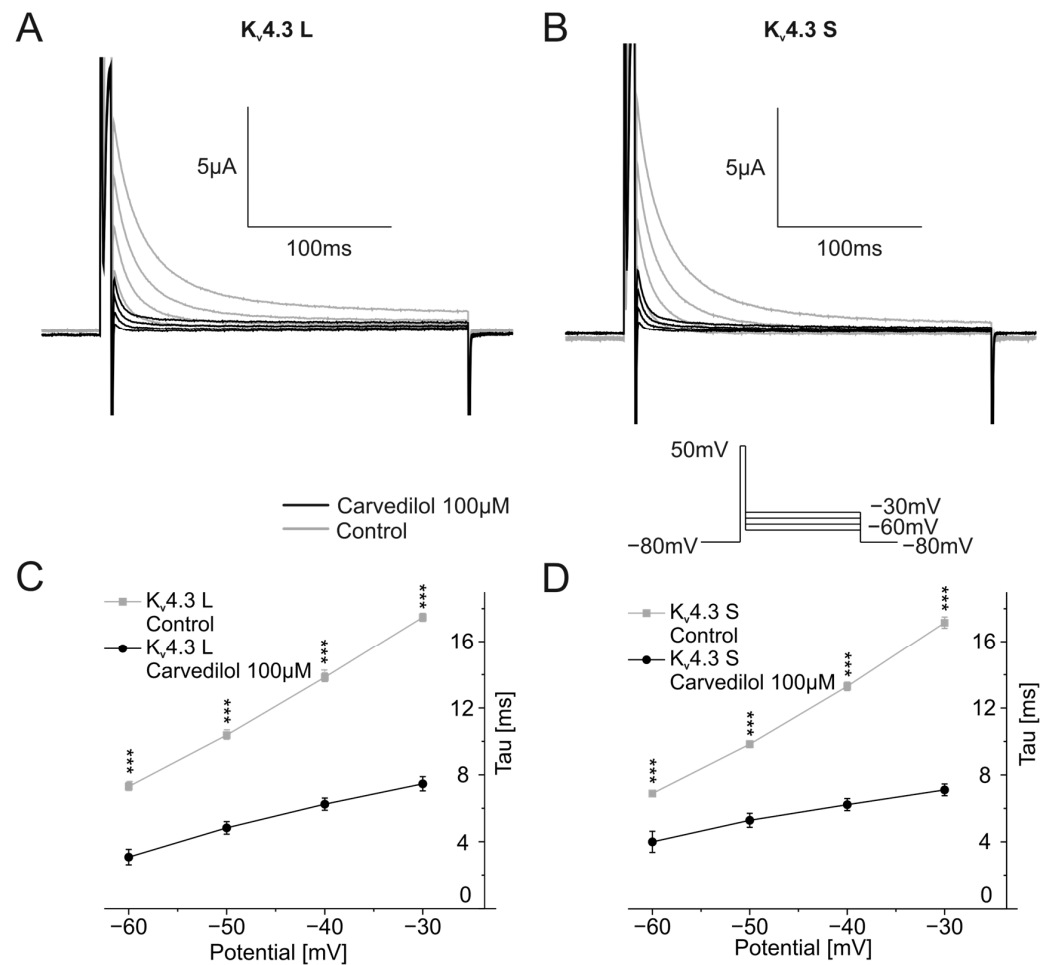


**Figure 5.** Effects of carvedilol (100 μM) on deactivation of  $K_v4.3$  isoforms. (A,B) Representative current traces of  $K_v4.3$  L (A) and  $K_v4.3$  S (B) induced by indicated voltage protocol prior to (gray) and after (black) carvedilol application (50 min). (C,D) Deactivation time constants for  $K_v4.3$  L (C) and  $K_v4.3$  S (D) ( $n = 11$ ). \*\*\*  $p < 0.001$ .

### 2.3. Effects of Bisoprolol on $K_v4.3$ Channel Isoforms

The impact of the bisoprolol on currents carried by  $K_v4.3$  isoforms was analyzed as described earlier using a single step depolarizing voltage protocol. Example traces are depicted in Figure 6A,B. Bisoprolol neither affected  $K_v4.3$  L nor  $K_v4.3$  S current amplitudes (Figure 6A,B). Peak currents did not change significantly during the 50 min wash-in compared to control measurements for  $K_v4.3$  L ( $102.3 \pm 7.5\%$ ,  $n = 11$ ,  $p = 0.765$ ) or  $K_v4.3$  S ( $95.3 \pm 8.7\%$ ,  $n = 9$ ,  $p = 0.607$ ) (Figure 6C,D).

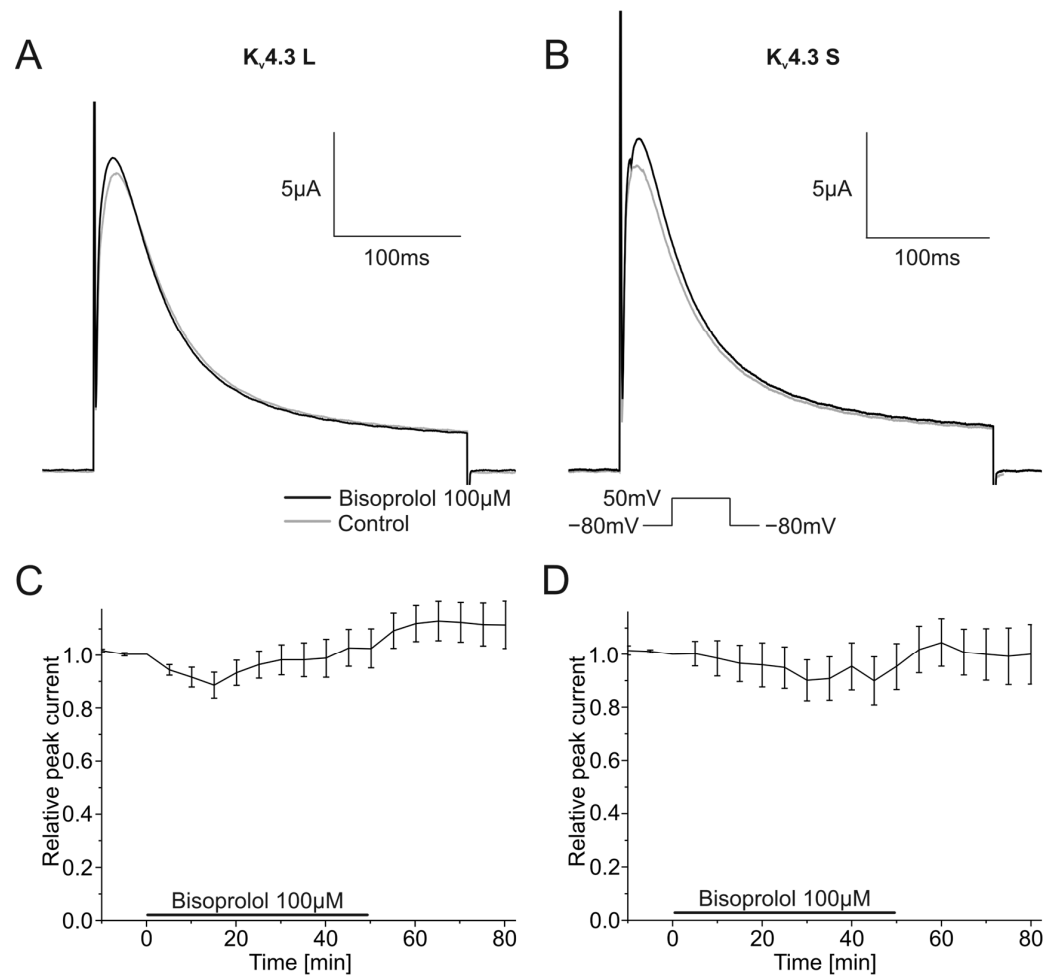


**Figure 6.** Effects of bisoprolol (100  $\mu\text{M}$ ) on  $\text{K}_v4.3$  isoforms. (A,B) Representative  $\text{K}_v4.3$  L (A) and  $\text{K}_v4.3$  S (B) current traces of prior to (gray) and after (black) bisoprolol application (50 min). (C,D) Relative peak current carried by  $\text{K}_v4.3$  L ( $n = 11$ ) (C) or  $\text{K}_v4.3$  S ( $n = 9$ ) (D) during application of 100  $\mu\text{M}$  bisoprolol.

#### 2.4. Effects of Metoprolol on the Function of $\text{K}_v4.3$ Channel Isoforms

Pharmacological effects of 100  $\mu\text{M}$  metoprolol on both  $\text{K}_v4.3$  isoforms were similarly assessed.  $\text{K}_v4.3$  L currents were blocked  $36.5 \pm 2.8\%$  ( $n = 9$ ,  $p < 0.001$ ), and  $\text{K}_v4.3$  S  $35.3 \pm 3.9\%$  ( $n = 9$ ,  $p < 0.001$ ) during metoprolol application (Figure 7A,B). The degree of current block did not differ between isoforms. Inhibitory effects of metoprolol on  $\text{K}_v4.3$  S appeared to be partially but not significantly reversible; mean peak  $\text{K}_v4.3$  S current normalized to control conditions recovered during 30 min wash-out from  $64.7 \pm 3.9\%$  in the presence of metoprolol to  $76.9 \pm 8.5\%$  ( $n = 9$ ) (Figure 7D). No apparent recovery was observed among  $\text{K}_v4.3$  L channels ( $63.5 \pm 2.8\%$  versus  $62.5 \pm 5.1\%$  after wash out,  $n = 9$ ) (Figure 7C).  $\text{IC}_{50}$  values for metoprolol blockade yielded  $47.3 \pm 34.2 \mu\text{M}$  ( $n = 9\text{--}11$ ) for  $\text{K}_v4.3$  L and  $49.8 \pm 0.7 \mu\text{M}$  for  $\text{K}_v4.3$  S ( $n = 9\text{--}11$ ), respectively (Figure 7E,F).

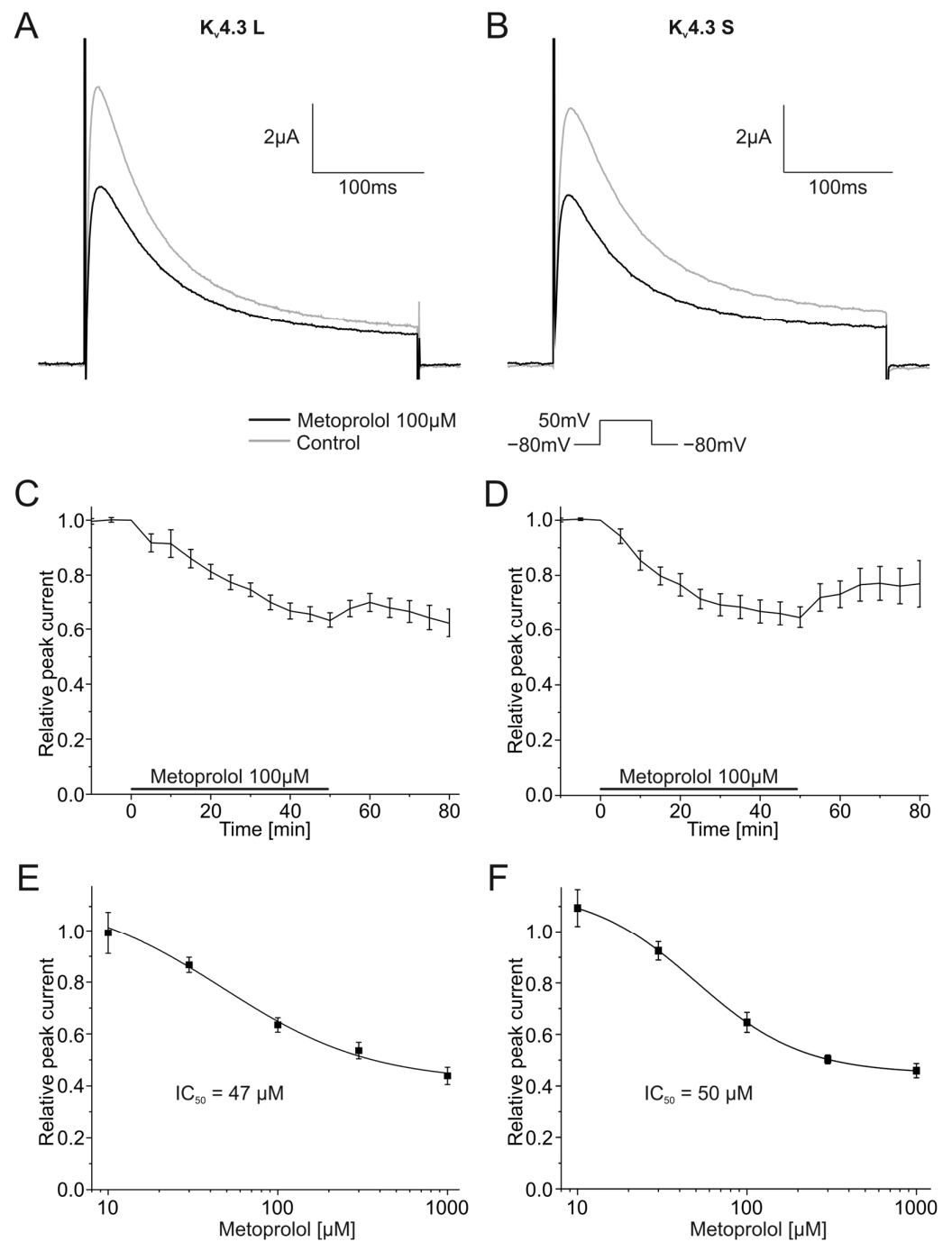


**Figure 7.** Effects of metoprolol (100 μM) on Kv4.3 currents. (A,B) Representative Kv4.3 L (A) and Kv4.3 S (B) current traces of prior to (gray) and after (black) metoprolol application (50 min). (C,D) Relative peak currents of Kv4.3 L ( $n = 9$ ) (C) and Kv4.3 S ( $n = 9$ ) (D) before, during and after application of 100 μM metoprolol. (E,F) Concentration-response curves for Kv4.3 L ( $n = 9-11$ ) ( $IC_{50} = 47.3 \pm 34.2 \mu\text{M}$ ) (E) and Kv4.3 S ( $n = 9-11$ ) ( $IC_{50} = 49.8 \pm 0.7 \mu\text{M}$ ) (F).

### 2.5. Effects of Betablockers on the Expression of Kv4.3 Isoforms in HEK Cells

To study the effects of the betablockers on the expression of Kv4.3 protein, both isoforms were individually expressed in HEK-293T cells (Figure 8A,B). Expression of Kv4.3 L and Kv4.3 S whole cell protein was not significantly reduced after incubation with betablockers bisoprolol, carvedilol, or metoprolol, respectively (Figure 8C,D). Protein content relative to control levels were  $68.9 \pm 6.8\%$  for bisoprolol ( $n = 6$ ,  $p = 0.180$ ),  $64.0 \pm 7.8\%$  for carvedilol ( $n = 6$ ,  $p = 0.082$ ) and  $71.2 \pm 6.6\%$  for metoprolol ( $n = 6$ ,  $p = 0.257$ ) for Kv4.3 L without reach-

ing statistical significance. For the  $K_v4.3 S$  isoform, protein expression relative to control yielded  $85.1 \pm 7.6\%$  for bisoprolol ( $n = 6, p = 1$ ),  $77.0 \pm 6.1\%$  for carvedilol ( $n = 6, p = 1$ ), and  $94.2 \pm 14.2\%$  for metoprolol ( $n = 6, p = 1$ ) without reaching statistical significance.

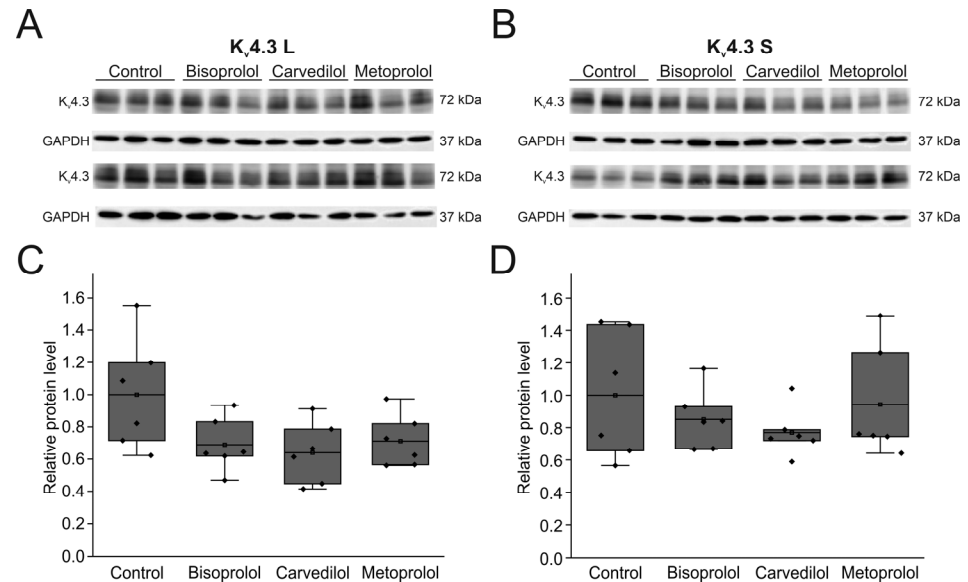


**Figure 8.** Effects of betablockers on  $K_v4.3$  isoform expression in HEK-293T cells. (A) Representative Western blots after transfection with  $K_v4.3 L$  (A) or  $K_v4.3 S$  (B) before and after incubation with respective betablockers (100  $\mu M$ ) for 24 h ( $n = 6$  each). (C,D) Protein quantification of  $K_v4.3 L$  (C) and  $K_v4.3 S$  (D) protein relative to respective controls and normalized to GAPDH.

### 3. Discussion

Carvedilol and metoprolol significantly blocked two cardiac  $K_v4.3$  channels isoforms that contribute to repolarization of the cardiac action potential. By contrast, bisoprolol did not affect  $K_v4.3$  currents, indicating drug-specific actions of carvedilol and metoprolol.

#### 3.1. Mechanisms of Block

The rapid development of the block after application of metoprolol and carvedilol indicates a direct interaction between the drug molecules and the respective  $K_v4.3$  isoforms as the primary molecular mechanism of action. This assumption is reinforced by changes in biophysical characteristics of the  $K_v4.3$  current after application of carvedilol. It has been shown that pre-pulse duration affects  $K_v4.3$  inactivation kinetics [23]. Thus, we compared longer (2000 ms) pre-pulses to shorter (200 ms) voltage steps assuming faster heart rates during arrhythmia, revealing rate-independent inhibition of  $K_v4.3 L$  and  $K_v4.3 S$  isoforms by carvedilol.

$K_v4.3 L$  is upregulated and  $K_v4.3 S$  is downregulated in HF [4]. Therefore, an  $I_{to}$ -targeting antiarrhythmic drug therapy should ideally target the  $K_v4.3 L$  isoform. There were no pronounced differences between the effects on  $K_v4.3 L$  and  $K_v4.3 S$  currents for any of the studied betablockers and biophysical parameters. We conclude from these findings that metoprolol and carvedilol cause  $K_v4.3$  current inhibition of both isoforms via the same molecular mechanism(s). The  $K_v4.3 L$  type isoform differs from the S isoform in a 19 amino acid long sequence at the C-terminal, intracellular end of the channel [12,13]. This portion of the protein harbors a PKC phosphorylation site. We cannot exclude those indirect differential effects of betablockers on  $K_v4.3$  isoforms via adrenergic signaling pathways under adrenergic stimulation that are beyond scope of this study.

Bisoprolol and metoprolol counteracted the decreased  $K_v4.3$  expression and the concomitant reduction of  $I_{to}$  in different HF animal models [24,25]. In our in vitro analysis, the incubation of transfected HEK cells with the respective betablockers did not affect expression levels of the respective  $K_v4.3$  isoforms. It should be noted that HEK-293T

cells endogenously express alpha-1 adrenoceptors [26], and even potentially possible adrenoceptor-blocking effects did not change expression levels.

### 3.2. Clinical Significance

Betablockers bisoprolol, carvedilol, and metoprolol exert a class effect during treatment of HF patients with reduced ejection fraction, with no apparent evidence for the superiority of any single agent over the others [14,27]. However, additional inhibition of potassium channels may suppress cardiac arrhythmias through prolongation of the action potential and by preventing electrical reentry. Multi-channel blocking effects of carvedilol may contribute to these antiarrhythmic effects [18–22]. Indeed, carvedilol was superior to metoprolol in small studies in reducing ICD therapies for ventricular arrhythmias [28] and in avoiding inappropriate ICD therapies [29].

Inhibition of  $K_v4.3$  channels by carvedilol or to lesser extent metoprolol could thus exert beneficial antiarrhythmic effects. The drug concentrations used in our study are apparently higher when compared to the maximum therapeutic plasma concentrations:  $IC_{50}$  values of  $57.1 \pm 12.6 \mu\text{M}$  (L isoform) and  $58.2 \pm 6.2 \mu\text{M}$  (S isoform) were obtained for carvedilol. During therapeutic application of carvedilol, maximum plasma concentrations ranging from 0.1–0.6  $\mu\text{M}$  were measured [20] (Table S1 in Supplementary Material). However, compared to mammalian cells, the concentrations for pharmacological ion channel inhibition in *Xenopus laevis* oocytes tend to be about 5 to 10 times higher [30], indicating that carvedilol effects observed here may be physiologically relevant during drug use in humans.

### 3.3. Potential Limitations

This study focused on acute, direct effects of betablockers on  $K_v4.3$  channels. Potential pharmacological effects on other subunits of  $I_{to}$  such as  $K_{chip2}$  were not analyzed. In addition, other mechanisms beyond direct channel binding were not assessed and need to be investigated in future studies, and cardiac cell lines must be modified to assess isoform specific  $K_v4.3$  characteristics [31,32]. In contrast to human ventricular cardiomyocytes in heart failure [4,33], differential  $K_v4.3$  isoform expression and remodeling has not been assessed in cardiac cell lines so far. Finally, clinical consequences and the potential differential effect on arrhythmias would have to be investigated in clinical trials with head-to-head comparisons.

## 4. Materials and Methods

### 4.1. Drugs

Bisoprolol was dissolved in 87% distilled water and 13% dimethyl sulfoxide, carvedilol in 24% distilled water and 76% dimethyl sulfoxide, and metoprolol in distilled water. The betablockers were stored as 100 mM stock solutions for electrophysiological measurements, and as 10 mM stock solutions for the experiments involving HEK cells at room temperature. For the experiments, stock solutions were diluted to the required concentrations.

### 4.2. Animal Handling and Ethics Statement

Animal studies were performed in compliance with the Guide for the Care and Use of Laboratory Animals, as approved and published by the U.S. National Institutes of Health (NIH publication No. 85–23, revised 1985) as well as the current version of the German Law on the Protection of Animals. The investigation conforms to the Directive 2010/63/EU of the European parliament. Surgical procedures on female *Xenopus laevis* frogs were institutionally approved (35-9185.81/G-270/17) and performed as previously reported [34].

### 4.3. Expression of $K_v4.3$ Channel Isoforms in *Xenopus Laevis* Oocytes

DNA encoding  $K_v4.3$  isoforms L and S were introduced into DH5- $\alpha$  bacteria with the help of the plasmid vector pMAX<sup>-</sup>. Plasmid DNA was then isolated using the QIAprep Spin Miniprep Kit (Qiagen, Hilden, Germany) and linearized using PmeI. Next, the DNA

was transcribed using T7 DNA polymerase and the mMessage mMachine Kit (Ambion, Austin, TX, USA). The concentration of the transcribed RNA was determined using NanoDrop 2000 (Thermo Fisher Scientific, Waltham, MA, USA). The RNA was then injected into stages V and VI defolliculated *Xenopus laevis* oocytes using a Nanoinjector (Nanoject II, H. Saur, Reutlingen, Germany). The injected volume was 46 nl and the concentration of injected cRNA was 10 ng. The electrophysiological measurements were carried out 2–3 days after the injection.

#### 4.4. Expression of $K_v4.3$ Channel Isoforms in HEK Cell Line

Human embryonic kidney (HEK-293T) cells were cultured at 37 °C with 5% CO<sub>2</sub>. HEK cells were transfected with the 1 µg DNA of  $K_v4.3$  L and S per well using the Lipofectamine™3000 Transfection reagent (Invitrogen, Thermo Fisher Scientific Inc. Carlsbad, CA, USA). Twenty-four hours after transfection, the cells were incubated with 10 µM of the different betablockers for another 24 h.

#### 4.5. Voltage-Clamp Electrophysiology

Two to three days after RNA injection, the electrophysiological measurements were performed using the two-voltage electrode clamp technique as described before [35]. Currents were recorded using an Oocyte Clamp amplifier (Warner OC-725A, Warner Instruments, Hamden, CT, USA) and Pclamp software version 8.2 (Axon Instruments, Foster City, CA, USA). Data were sampled at 2 kHz and filtered at 1 kHz. Voltage clamp electrodes were pulled from glass capillaries (GB100F-10, Science Products GmbH, Hofheim, Germany) using a micropipette puller (P-1000 Next Generation Micropipette Puller, Sutter Instrument, Novato, CA, USA) filled with 3 M of KCl solution; the electrodes had tip resistances were 5–10 MΩ. The standard extracellular bath solution contained 96 mM NaCl, 4 mM KCl, 1.1 mM CaCl<sub>2</sub>, 1 mM MgCl<sub>2</sub> and 5 mM HEPES and was adjusted to pH 7.4 with NaOH. Before the measurements, the oocytes were preincubated in this solution for at least 20 min. The experiments were carried out under steady gravity-driven perfusion at room temperature.

$K_v4.3$  currents were induced with a single depolarizing voltage step from a holding potential of −80 mV to +50 mV for 250 ms. To evaluate the effect of 100 µM carvedilol on  $K_v4.3$  current, oocytes were first treated with the betablocker for 50 min, followed by washout with a 4 mM K<sup>+</sup> solution to assess reversibility. Values of measured peak amplitudes were normalized to the value of the peak amplitude obtained during the last measurement prior to drug application.

#### 4.6. Western Blots

For Western Blot studies, HEK cells were lysed in a radioimmunoprecipitation (RIPA) buffer consisting of 20 mM Tris-HCl, 0.5% NP-40, 0.5% sodium-deoxycholate, 150 mM NaCl, 1 mM EDTA, 1 mM Na<sub>3</sub>VO<sub>4</sub>, 1 mM NaF and inhibitors proteases (CompleteMini, Roche Applied Science, Indianapolis, IN, USA). Those lysed cells were incubated on ice for 20 min and then centrifugated for 30 min at 14,000 × g and 4 °C. The supernatants were then collected, and the protein concentration was determined using the bicinchoninic acid (BCA) protein assay (Thermo Scientific, Rockford, IL, USA). The proteins were then diluted to equal concentrations with water. Next, equal amounts of proteins were separated on a 10% SDS polyacrylamide gel and then transferred onto polyvinylidene difluoride membranes (Amersham™ Protran R Western blotting membranes, nitrocellulose, Cytiva, Marlborough, MA, USA). After being blocked with 5% milk in PBST for 2 h at room temperature, those membranes were incubated with primary antibodies directed against  $K_v4.3$  (1:1000 dilution, #APC-017, rabbit, Alomone Lab, Jerusalem, Israel) at 4 °C overnight. As a control, the respective control peptides for  $K_v4.3$ , supplied by the company, were used (BLP-PC017, Alomone Lab, Jerusalem, Israel). A secondary antibody donkey-anti-rabbit (1:3000 dilution, ab6802, Abcam, Cambridge, UK) was used. Signals were developed using the Azure 600 Ultimate Western Imaging (Azure Biosystems, Dublin, CA, USA) and

ECL™ Select Western Blotting Detection Reagent (Cytiva, Marlborough, MA, USA). After removal of the primary and secondary antibodies (ReBlot Strong Stripping Solution, Merck, Germany), the membranes were incubated in anti-GAPDH primary antibodies (1:20,000, ab181602, Abcam, Cambridge, UK) and the corresponding secondary donkey-anti-rabbit antibody (1:3000 dilution, ab6802, Abcam, Cambridge, UK). Optical density was quantified using ImageJ 1.50i Software (National Institutes of Health, Bethesda, MD, USA).

#### 4.7. Data Analysis and Statistics

Data was analyzed using Origin2022 software (OriginLab, Northampton, MA, USA) and Microsoft Excel software 2021 (Microsoft, Redmond, WA, USA). Data are expressed as mean  $\pm$  standard error of the mean (SEM). The concentration response curve was fitted with a Hill1 function ( $y = \text{START} + ((\text{END} - \text{START}) x^n) / (k^n + x^n)$ ). Curves for activation and inactivation were fitted with a Boltzmann function ( $y = A2 + (A1 - A2) / (1 + \exp((x - x_0) / dx))$ ). Current traces for the deactivation measurements were fitted with a one-phase exponential decay function with time constant parameter (ExpDec1) ( $y = y_0 + Ae^{-x/t}$ ). Curves for the recovery measurements were fitted with a one-phase exponential association equation (ExpAssoc1) ( $y = Yb + A \times (1 - e^{-(x-TD)/\text{Tau}}$ ). Kolmogorov–Smirnov tests were used to confirm normal distribution of the data. To test the statistical significance, paired Student's *t*-tests were applied for all the electrophysiological measurements. For the statistical analysis of the Western Blots, ANOVA tests were used.  $p < 0.05$  was considered statistically significant.

## 5. Conclusions

Widely used cardioselective betablockers exert differential effects on cardiac repolarizing  $K_v4.3$  channels underlying the  $I_{to}$  current. Carvedilol has a strong inhibitory effect on the  $K_v4.3$  isoforms, whereas metoprolol was less effective. Concentrations required for blockade were within upper physiological ranges. Bisoprolol did not have any effect on  $K_v4.3$  currents. Specific electropharmacological actions of carvedilol and metoprolol may be considered when choosing betablockers for HF therapy.

**Supplementary Materials:** The following supporting information can be downloaded at: <https://www.mdpi.com/article/10.3390/ijms241813842/s1>. References [36–57] are cited in the Supplementary Materials.

**Author Contributions:** Conceptualization, A.-K.R. and D.T.; Data curation, A.-K.R., J.H., M.E.M., J.P., H.G. and F.P.; Formal analysis, A.-K.R. and J.H.; Funding acquisition, A.-K.R.; Investigation, A.-K.R. and J.H.; Methodology, A.-K.R. and J.H.; Project administration, A.-K.R.; Resources, A.-K.R., N.F. and D.T.; Software, A.-K.R. and D.T.; Supervision, A.-K.R. and D.T.; Validation, A.-K.R., J.H. and D.T.; Visualization, A.-K.R. and J.H.; Writing—original draft, A.-K.R. and J.H.; Writing—review and editing, A.-K.R., J.H., M.E.M., R.R., N.F., P.L. and D.T. All authors have read and agreed to the published version of the manuscript.

**Funding:** This research was funded in parts by Heidelberg University Medical School Olympia-Morata Grant to A.-K.R., the German Heart Foundation (Kaltenbach-Promotionstipendium to H.G.), and the Department of Cardiology (Cardiology-Career Program to J.H., F.P. and H.G.). J.H. and H.G. received funding from German Academic Scholarship Foundation.

**Institutional Review Board Statement:** 35-9185.81/G-270/17.

**Informed Consent Statement:** Not applicable.

**Data Availability Statement:** Raw data may be acquired from the corresponding author on reasonable request.

**Acknowledgments:** We gratefully acknowledge the excellent technical assistance of Axel Schöffel, Teresa Caspari, Patrizia Lo Vetere, Nicole Westerhorstmann and Miriam Baier.

**Conflicts of Interest:** The authors declare no conflict of interest.

## References

1. Dixon, J.E.; Shi, W.; Wang, H.S.; McDonald, C.; Yu, H.; Wymore, R.S.; Cohen, I.S.; McKinnon, D. Role of the Kv4.3 K<sup>+</sup> channel in ventricular muscle. A molecular correlate for the transient outward current. *Circ. Res.* **1996**, *79*, 659–668. [[CrossRef](#)]
2. Giudicessi, J.R.; Ye, D.; Tester, D.J.; Crotti, L.; Mugione, A.; Nesterenko, V.V.; Albertson, R.M.; Antzelevitch, C.; Schwartz, P.J.; Ackerman, M.J. Transient outward current (I<sub>to</sub>) gain-of-function mutations in the KCND3-encoded Kv4.3 potassium channel and Brugada syndrome. *Heart Rhythm.* **2011**, *8*, 1024–1032. [[CrossRef](#)] [[PubMed](#)]
3. Olesen, M.S.; Refsgaard, L.; Holst, A.G.; Larsen, A.P.; Grubb, S.; Haunso, S.; Svendsen, J.H.; Olesen, S.P.; Schmitt, N.; Calloe, K. A novel KCND3 gain-of-function mutation associated with early-onset of persistent lone atrial fibrillation. *Cardiovasc. Res.* **2013**, *98*, 488–495. [[CrossRef](#)] [[PubMed](#)]
4. Radicke, S.; Cotella, D.; Graf, E.M.; Banse, U.; Jost, N.; Varro, A.; Tseng, G.N.; Ravens, U.; Wettwer, E. Functional modulation of the transient outward current I<sub>to</sub> by KCNE beta-subunits and regional distribution in human non-failing and failing hearts. *Cardiovasc. Res.* **2006**, *71*, 695–703. [[CrossRef](#)] [[PubMed](#)]
5. Janse, M.J. Electrophysiological changes in heart failure and their relationship to arrhythmogenesis. *Cardiovasc. Res.* **2004**, *61*, 208–217. [[CrossRef](#)] [[PubMed](#)]
6. Walmsley, J.; Rodriguez, J.F.; Mirams, G.R.; Burrage, K.; Efimov, I.R.; Rodriguez, B. mRNA expression levels in failing human hearts predict cellular electrophysiological remodeling: A population-based simulation study. *PLoS ONE* **2013**, *8*, e56359. [[CrossRef](#)] [[PubMed](#)]
7. Beuckelmann, D.J.; Nabauer, M.; Erdmann, E. Alterations of K<sup>+</sup> currents in isolated human ventricular myocytes from patients with terminal heart failure. *Circ. Res.* **1993**, *73*, 379–385. [[CrossRef](#)]
8. Kaab, S.; Dixon, J.; Duc, J.; Ashen, D.; Nabauer, M.; Beuckelmann, D.J.; Steinbeck, G.; McKinnon, D.; Tomaselli, G.F. Molecular basis of transient outward potassium current downregulation in human heart failure: A decrease in Kv4.3 mRNA correlates with a reduction in current density. *Circulation* **1998**, *98*, 1383–1393. [[CrossRef](#)]
9. Li, G.R.; Lau, C.P.; Ducharme, A.; Tardif, J.C.; Nattel, S. Transmural action potential and ionic current remodeling in ventricles of failing canine hearts. *Am. J. Physiol. Heart Circ. Physiol.* **2002**, *283*, H1031–H1041. [[CrossRef](#)]
10. Rozanski, G.J.; Xu, Z.; Whitney, R.T.; Murakami, H.; Zucker, I.H. Electrophysiology of rabbit ventricular myocytes following sustained rapid ventricular pacing. *J. Mol. Cell Cardiol.* **1997**, *29*, 721–732. [[CrossRef](#)]
11. Tsuji, Y.; Opthof, T.; Kamiya, K.; Yasui, K.; Liu, W.; Lu, Z.; Kodama, I. Pacing-induced heart failure causes a reduction of delayed rectifier potassium currents along with decreases in calcium and transient outward currents in rabbit ventricle. *Cardiovasc. Res.* **2000**, *48*, 300–309. [[CrossRef](#)]
12. Kong, W.; Po, S.; Yamagishi, T.; Ashen, M.D.; Stetten, G.; Tomaselli, G.F. Isolation and characterization of the human gene encoding I<sub>to</sub>: Further diversity by alternative mRNA splicing. *Am. J. Physiol.* **1998**, *275*, H1963–H1970.
13. Ohya, S.; Tanaka, M.; Oku, T.; Asai, Y.; Watanabe, M.; Giles, W.R.; Imaizumi, Y. Molecular cloning and tissue distribution of an alternatively spliced variant of an A-type K<sup>+</sup> channel alpha-subunit, Kv4.3 in the rat. *FEBS Lett.* **1997**, *420*, 47–53. [[CrossRef](#)] [[PubMed](#)]
14. McDonagh, T.A.; Metra, M.; Adamo, M.; Gardner, R.S.; Baumbach, A.; Bohm, M.; Burri, H.; Butler, J.; Celutkiene, J.; Chioncel, O.; et al. 2021 ESC Guidelines for the diagnosis and treatment of acute and chronic heart failure. *Eur. Heart J.* **2021**, *42*, 3599–3726. [[CrossRef](#)] [[PubMed](#)]
15. The Cardiac Insufficiency Bisoprolol Study II (CIBIS-II): A randomised trial. *Lancet* **1999**, *353*, 9–13. [[CrossRef](#)]
16. Effect of metoprolol CR/XL in chronic heart failure: Metoprolol CR/XL Randomised Intervention Trial in Congestive Heart Failure (MERIT-HF). *Lancet* **1999**, *353*, 2001–2007. [[CrossRef](#)]
17. Packer, M.; Coats, A.J.; Fowler, M.B.; Katus, H.A.; Krum, H.; Mohacsi, P.; Rouleau, J.L.; Tendera, M.; Castaigne, A.; Roecker, E.B.; et al. Effect of carvedilol on survival in severe chronic heart failure. *N. Engl. J. Med.* **2001**, *344*, 1651–1658. [[CrossRef](#)] [[PubMed](#)]
18. Staudacher, K.; Staudacher, I.; Ficker, E.; Seyler, C.; Gierten, J.; Kisselbach, J.; Rahm, A.K.; Trappe, K.; Schweizer, P.A.; Becker, R.; et al. Carvedilol targets human K2P 3.1 (TASK1) K<sup>+</sup> leak channels. *Br. J. Pharmacol.* **2011**, *163*, 1099–1110. [[CrossRef](#)]
19. Kawakami, K.; Nagatomo, T.; Abe, H.; Kikuchi, K.; Takemasa, H.; Anson, B.D.; Delisle, B.P.; January, C.T.; Nakashima, Y. Comparison of HERG channel blocking effects of various beta-blockers—Implication for clinical strategy. *Br. J. Pharmacol.* **2006**, *147*, 642–652. [[CrossRef](#)]
20. Karle, C.A.; Kreye, V.A.; Thomas, D.; Rockl, K.; Kathofer, S.; Zhang, W.; Kiehn, J. Antiarrhythmic drug carvedilol inhibits HERG potassium channels. *Cardiovasc. Res.* **2001**, *49*, 361–370. [[CrossRef](#)]
21. El-Sherif, N.; Turitto, G. Electrophysiologic effects of carvedilol: Is carvedilol an antiarrhythmic agent? *Pacing Clin. Electrophysiol.* **2005**, *28*, 985–990. [[CrossRef](#)] [[PubMed](#)]
22. Kisselbach, J.; Seyler, C.; Schweizer, P.A.; Gerstberger, R.; Becker, R.; Katus, H.A.; Thomas, D. Modulation of K2P 2.1 and K2P 10.1 K<sup>+</sup> channel sensitivity to carvedilol by alternative mRNA translation initiation. *Br. J. Pharmacol.* **2014**, *171*, 5182–5194. [[CrossRef](#)]
23. Wang, S.; Bondarenko, V.E.; Qu, Y.J.; Bett, G.C.; Morales, M.J.; Rasmusson, R.L.; Strauss, H.C. Time- and voltage-dependent components of Kv4.3 inactivation. *Biophys. J.* **2005**, *89*, 3026–3041. [[CrossRef](#)] [[PubMed](#)]
24. Li, X.; Wang, T.; Han, K.; Zhuo, X.; Lu, Q.; Ma, A. Bisoprolol reverses down-regulation of potassium channel proteins in ventricular tissues of rabbits with heart failure. *J. Biomed. Res.* **2011**, *25*, 274–279. [[CrossRef](#)] [[PubMed](#)]
25. Rossow, C.F.; Minami, E.; Chase, E.G.; Murry, C.E.; Santana, L.F. NFATc3-induced reductions in voltage-gated K<sup>+</sup> currents after myocardial infarction. *Circ. Res.* **2004**, *94*, 1340–1350. [[CrossRef](#)]

26. Atwood, B.K.; Lopez, J.; Wager-Miller, J.; Mackie, K.; Straiker, A. Expression of G protein-coupled receptors and related proteins in HEK293, AtT20, BV2, and N18 cell lines as revealed by microarray analysis. *BMC Genom.* **2011**, *12*, 14. [[CrossRef](#)]
27. Ahmed, A.A.E. Perspective on the Role of Four Beta-blockers in Heart Failure. *Curr. Rev. Clin. Exp. Pharmacol.* **2022**, *17*, 85–89. [[CrossRef](#)]
28. Ayan, M.; Habash, F.; Alqam, B.; Gheith, Z.; Cross, M.; Vallurupalli, S.; Paydak, H. A comparison of anti-arrhythmic efficacy of carvedilol vs. metoprolol succinate in patients with implantable cardioverter-defibrillators. *Clin. Cardiol.* **2019**, *42*, 299–304. [[CrossRef](#)]
29. Ruwald, M.H.; Abu-Zeitone, A.; Jons, C.; Ruwald, A.C.; McNitt, S.; Kutuyifa, V.; Zareba, W.; Moss, A.J. Impact of carvedilol and metoprolol on inappropriate implantable cardioverter-defibrillator therapy: The MADIT-CRT trial (Multicenter Automatic Defibrillator Implantation with Cardiac Resynchronization Therapy). *J. Am. Coll. Cardiol.* **2013**, *62*, 1343–1350. [[CrossRef](#)]
30. Rolf, S.; Haverkamp, W.; Borggreffe, M.; Musshoff, U.; Eckardt, L.; Mergenthaler, J.; Snyders, D.J.; Pongs, O.; Speckmann, E.J.; Breithardt, G.; et al. Effects of antiarrhythmic drugs on cloned cardiac voltage-gated potassium channels expressed in *Xenopus* oocytes. *Naunyn Schmiedebergs Arch. Pharmacol.* **2000**, *362*, 22–31. [[CrossRef](#)]
31. Shen, A.; Chen, D.; Kaur, M.; Bartels, P.; Xu, B.; Shi, Q.; Martinez, J.M.; Man, K.M.; Nieves-Cintrón, M.; Hell, J.W.; et al. beta-blockers augment L-type Ca<sup>2+</sup> channel activity by targeting spatially restricted beta(2)AR signaling in neurons. *Elife* **2019**, *8*, e49464. [[CrossRef](#)] [[PubMed](#)]
32. Li, Y.; Duan, H.; Yi, J.; Wang, G.; Cheng, W.; Feng, L.; Liu, J. Kv4.2 phosphorylation by PKA drives Kv4.2-KChIP2 dissociation, leading to Kv4.2 out of lipid rafts and internalization. *Am. J. Physiol. Cell Physiol.* **2022**, *323*, C190–C201. [[CrossRef](#)]
33. Rahm, A.-K.; Müller, M.E.; Gramlich, D.; Lugenbiel, P.; Uludag, E.; Rivinius, R.; Ullrich, N.D.; Schmack, B.; Ruhparwar, A.; Heimerger, T.; et al. Inhibition of cardiac Kv4.3 (Ito) channel isoforms by class I antiarrhythmic drugs lidocaine and mexiletine. *Eur. J. Pharmacol.* **2020**, *880*, 173915. [[CrossRef](#)]
34. Rahm, A.K.; Gierten, J.; Kisselbach, J.; Staudacher, I.; Staudacher, K.; Schweizer, P.A.; Becker, R.; Katus, H.A.; Thomas, D. PKC-dependent activation of human K(2P) 18.1 K<sup>+</sup> channels. *Br. J. Pharmacol.* **2012**, *166*, 764–773. [[CrossRef](#)] [[PubMed](#)]
35. Kiehn, J.; Thomas, D.; Karle, C.A.; Schols, W.; Kubler, W. Inhibitory effects of the class III antiarrhythmic drug amiodarone on cloned HERG potassium channels. *Naunyn Schmiedebergs Arch. Pharmacol.* **1999**, *359*, 212–219. [[CrossRef](#)]
36. Packer, M.; Lukas, M.A.; Tenero, D.M.; Baidoo, C.A.; Greenberg, B.H.; Study, G. Pharmacokinetic profile of controlled-release carvedilol in patients with left ventricular dysfunction associated with chronic heart failure or after myocardial infarction. *Am. J. Cardiol.* **2006**, *98*, 39L–45L. [[CrossRef](#)] [[PubMed](#)]
37. Tenero, D.; Boike, S.; Boyle, D.; Ilson, B.; Fesniak, H.F.; Brozena, S.; Jorkasky, D. Steady-state pharmacokinetics of carvedilol and its enantiomers in patients with congestive heart failure. *J. Clin. Pharmacol.* **2000**, *40*, 844–853. [[CrossRef](#)]
38. Gehr, T.W.; Tenero, D.M.; Boyle, D.A.; Qian, Y.; Sica, D.A.; Shusterman, N.H. The pharmacokinetics of carvedilol and its metabolites after single and multiple dose oral administration in patients with hypertension and renal insufficiency. *Eur. J. Clin. Pharmacol.* **1999**, *55*, 269–277. [[CrossRef](#)] [[PubMed](#)]
39. do Carmo Borges, N.C.; Mendes, G.D.; de Oliveira Silva, D.; Marcondes Rezende, V.; Barrientos-Astigarraga, R.E.; De Nucci, G. Quantification of carvedilol in human plasma by high-performance liquid chromatography coupled to electrospray tandem mass spectrometry: Application to bioequivalence study. *J. Chromatogr. B Analyt Technol. Biomed. Life Sci.* **2005**, *822*, 253–262. [[CrossRef](#)]
40. Stout, S.M.; Nielsen, J.; Bleske, B.E.; Shea, M.; Brook, R.; Kerber, K.; Welage, L.S. The impact of paroxetine coadministration on stereospecific carvedilol pharmacokinetics. *J. Cardiovasc. Pharmacol. Ther.* **2010**, *15*, 373–379. [[CrossRef](#)]
41. Kim, Y.H.; Choi, H.Y.; Noh, Y.H.; Lee, S.H.; Lim, H.S.; Kim, C.; Bae, K.S. Dose proportionality and pharmacokinetics of carvedilol sustained-release formulation: A single dose-ascending 10-sequence incomplete block study. *Drug Des. Devel Ther.* **2015**, *9*, 2911–2918.
42. Kendall, M.J.; John, V.A.; Quarterman, C.P.; Welling, P.G. A single and multiple dose pharmacokinetic and pharmacodynamic comparison of conventional and slow-release metoprolol. *Eur. J. Clin. Pharmacol.* **1980**, *17*, 87–92. [[CrossRef](#)] [[PubMed](#)]
43. Quarterman, C.P.; Kendall, M.J.; Jack, D.B. The effect of age on the pharmacokinetics of metoprolol and its metabolites. *Br. J. Clin. Pharmacol.* **1981**, *11*, 287–294. [[CrossRef](#)] [[PubMed](#)]
44. Kendall, M.J.; Quarterman, C.P.; Jack, D.B.; Beeley, L. Metoprolol pharmacokinetics and the oral contraceptive pill. *Br. J. Clin. Pharmacol.* **1982**, *14*, 120–122. [[CrossRef](#)] [[PubMed](#)]
45. Burke, S.K.; Amin, N.S.; Incerti, C.; Plone, M.A.; Lee, J.W. Sevelamer hydrochloride (Renagel), a phosphate-binding polymer, does not alter the pharmacokinetics of two commonly used antihypertensives in healthy volunteers. *J. Clin. Pharmacol.* **2001**, *41*, 199–205. [[CrossRef](#)] [[PubMed](#)]
46. Werner, U.; Werner, D.; Rau, T.; Fromm, M.F.; Hinz, B.; Brune, K. Celecoxib inhibits metabolism of cytochrome P450 2D6 substrate metoprolol in humans. *Clin. Pharmacol. Ther.* **2003**, *74*, 130–137. [[CrossRef](#)] [[PubMed](#)]
47. Aqil, M.; Ali, A.; Sultana, Y.; Saha, N. Comparative bioavailability of metoprolol tartrate after oral and transdermal administration in healthy male volunteers. *Clin. Drug Investig.* **2007**, *27*, 833–839. [[CrossRef](#)]
48. Turpault, S.; Brian, W.; Van Horn, R.; Santoni, A.; Poitiers, F.; Donazzolo, Y.; Boulenc, X. Pharmacokinetic assessment of a five-probe cocktail for CYPs 1A2, 2C9, 2C19, 2D6 and 3A. *Br. J. Clin. Pharmacol.* **2009**, *68*, 928–935. [[CrossRef](#)]
49. Krauwinkel, W.; Dickinson, J.; Schaddelee, M.; Meijer, J.; Tretter, R.; van de Wetering, J.; Strabach, G.; van Gelderen, M. The effect of mirabegron, a potent and selective beta3-adrenoceptor agonist, on the pharmacokinetics of CYP2D6 substrates desipramine and metoprolol. *Eur. J. Drug Metab. Pharmacokinet.* **2014**, *39*, 43–52. [[CrossRef](#)]

50. Garimella, T.; Tao, X.; Sims, K.; Chang, Y.T.; Rana, J.; Myers, E.; Wind-Rotolo, M.; Bhatnagar, R.; Eley, T.; LaCreta, F.; et al. Effects of a Fixed-Dose Co-Formulation of Daclatasvir, Asunaprevir, and Beclabuvir on the Pharmacokinetics of a Cocktail of Cytochrome P450 and Drug Transporter Substrates in Healthy Subjects. *Drugs R D* **2018**, *18*, 55–65. [[CrossRef](#)]
51. Pfannenstiel, P.; Rummeny, E.; Baew-Christow, T.; Bux, B.; Cordes, M.; Adam, W.; Panitz, N.; Pabst, J.; Disselhoff, G. Pharmacokinetics of bisoprolol and influence on serum thyroid hormones in hyperthyroid patients. *J. Cardiovasc. Pharmacol.* **1986**, *8* (Suppl. 11), S100–S105. [[CrossRef](#)] [[PubMed](#)]
52. Hayes, P.C.; Jenkins, D.; Vavianos, P.; Dagap, K.; Johnston, A.; Ioannides, C.; Thomas, P.; Williams, R. Single oral dose pharmacokinetics of bisoprolol 10 mg in liver disease. *Eur. Heart J.* **1987**, *8* (Suppl. M), 23–29. [[CrossRef](#)] [[PubMed](#)]
53. Dutta, A.; Lanc, R.; Begg, E.; Robson, R.; Sia, L.; Dukart, G.; Desjardins, R.; Yacobi, A. Dose proportionality of bisoprolol enantiomers in humans after oral administration of the racemate. *J. Clin. Pharmacol.* **1994**, *34*, 829–836. [[CrossRef](#)] [[PubMed](#)]
54. Tjandrawinata, R.R.; Setiawati, E.; Yunaidi, D.A.; Santoso, I.D.; Setiawati, A.; Susanto, L.W. Bioequivalence study of two formulations of bisoprolol fumarate film-coated tablets in healthy subjects. *Drug Des. Devel Ther.* **2012**, *6*, 311–316. [[PubMed](#)]
55. Bus-Kwasnik, K.; Rudzki, P.J.; Ksycinska, H.; Les, A.; Serafin-Byczak, K.; Raszek, J.; Bielak, A.; Wybraniec, A.; Platek, A.E.; Szymanski, F.M.; et al. Bioequivalence study of 2.5 mg film-coated bisoprolol tablets in healthy volunteers. *Kardiol. Pol.* **2017**, *75*, 48–54. [[CrossRef](#)] [[PubMed](#)]
56. Kirch, W.; Rose, I.; Klingmann, I.; Pabst, J.; Ohnhaus, E.E. Interaction of bisoprolol with cimetidine and rifampicin. *Eur. J. Clin. Pharmacol.* **1986**, *31*, 59–62. [[CrossRef](#)]
57. Kirch, W.; Rose, I.; Demers, H.G.; Leopold, G.; Pabst, J.; Ohnhaus, E.E. Pharmacokinetics of bisoprolol during repeated oral administration to healthy volunteers and patients with kidney or liver disease. *Clin. Pharmacokinet.* **1987**, *13*, 110–117. [[CrossRef](#)]

**Disclaimer/Publisher’s Note:** The statements, opinions and data contained in all publications are solely those of the individual author(s) and contributor(s) and not of MDPI and/or the editor(s). MDPI and/or the editor(s) disclaim responsibility for any injury to people or property resulting from any ideas, methods, instructions or products referred to in the content.